ICHEP94 Ref. GLS0242
Submitted to PA 16 Pl 9

CLEO CONF 94-24
July 19, 1994

Measurement of $\mathcal{B}(\tau^- \to \nu_\tau K^- K^\circ)$ and $\mathcal{B}(\tau^- \to \nu_\tau K^- K^\circ \pi^\circ)$

J. Gronberg,[1] R. Kutschke,[1] S. Menary,[1] R.J. Morrison,[1] S. Nakanishi,[1] H.N. Nelson,[1] T.K. Nelson,[1] C. Qiao,[1] J.D. Richman,[1] A. Ryd,[1] D. Sperka,[1] H. Tajima,[1] M.S. Witherell,[1] R. Balest,[2] K. Cho,[2] W.T. Ford,[2] D.R. Johnson,[2] K. Lingel,[2] M. Lohner,[2] P. Rankin,[2] J.G. Smith,[2] J.P. Alexander,[3] C. Bebek,[3] K. Berkelman,[3] K. Bloom,[3] T.E. Browder,[3*] D.G. Cassel,[3] H.A. Cho,[3] D.M. Coffman,[3] D.S. Crowcroft,[3] P.S. Drell,[3] D. Dumas,[3] R. Ehrlich,[3] R. S. Galik,[3] P. Gaidarev,[3] M. Garcia-Sciveres,[3] B. Geiser,[3] B. Gittelman,[3] S.W. Gray,[3] D.L. Hartill,[3] B.K. Heltsley,[3] S. Henderson,[3] C.D. Jones,[3] S.L. Jones,[3] J. Kandaswamy,[3] N. Katayama,[3] P.C. Kim,[3] D.L. Kreinick,[3] G.S. Ludwig,[3] J. Masui,[3] J. Mevissen,[3] N.B. Mistry,[3] C.R. Ng,[3] E. Nordberg,[3] J.R. Patterson,[3] D. Peterson,[3] D. Riley,[3] S. Salman,[3] M. Sapper,[3] F. Würthwein,[3] P. Avery,[4] A. Freyberger,[4] J. Rodriguez,[4] S. Yang,[4] J. Yelton,[4] D. Cinabro,[5] T. Liu,[5] M. Saulnier,[5] R. Wilson,[5] H. Yamamoto,[5] T. Bergfeld,[6] B.I. Eisenstein,[6] G. Gollin,[6] B. Ong,[6] M. Palmer,[6] M. Selen,[6] J. J. Thaler,[6] K.W. Edwards,[7] M. Ogg,[7] A. Bellerive,[8] D.I. Britton,[8] E.R.F. Hyatt,[8] D.B. MacFarlane,[8] P.M. Patel,[8] B. Spaan,[8] A.J. Sadoff,[9] R. Ammar,[10] P. Baringer,[10] A. Bean,[10] D. Besson,[10] D. Coppage,[10] N. Copty,[10] R. Davis,[10] N. Hancock,[10] M. Kelly,[10] S. Kotov,[10] I. Kravchenko,[10] N. Kwak,[10] H. Lam,[10] Y. Kubota,[11] M. Lattery,[11] M. Momayezi,[11] J.K. Nelson,[11] S. Patton,[11] R. Poling,[11] V. Savinov,[11] S. Schrenk,[11] R. Wang,[11] M.S. Alam,[12] I.J. Kim,[12] Z. Ling,[12] A.H. Mahmood,[12] J.J. O'Neill,[12] H. Severini,[12] C.R. Sun,[12] F. Wappler,[12] G. Crawford,[13] C. M. Daubenmier,[13] R. Fulton,[13] D. Fujino,[13] K.K. Gan,[13] K. Honscheid,[13] H. Kagan,[13] R. Kass,[13] J. Lee,[13] R. Malchow,[13] M. Sung,[13] C. White,[13] M.M. Zoeller,[13] F. Butler,[14] X. Fu,[14] B. Nemati,[14] W.R. Ross,[14] P. Skubic,[14] M. Wood,[14] M. Bishai,[15] J. Fast,[15] E. Gerndt,[15] R.L. McIlwain,[15] T. Miao,[15] D.H. Miller,[15] M. Modesitt,[15] D. Payne,[15] E.I. Shibata,[15] I.P.J. Shipsey,[15] P.N. Wang,[15] M. Battle,[16] J. Ernst,[16] L. Gibbons,[16] Y. Kwon,[16] S. Roberts,[16] E.H. Thorndike,[16] C.H. Wang,[16] J. Dominick,[17] M. Lambrecht,[17] S. Sanghera,[17] V. Shelkov,[17] T. Skwarnicki,[17] R. Stroynowski,[17] I. Volobouev,[17] G. Wei,[17] P. Zadorozhny,[17] M. Artuso,[18] M. Gao,[18] M. Goldberg,[18] D. He,[18] N. Horwitz,[18] G.C. Moneti,[18] R. Mountain,[18] F. Muheim,[18] Y. Mukhin,[18] S. Playfer,[18] Y. Rozen,[18] S. Stone,[18] X. Xing,[18] G. Zhu,[18] J. Bartelt,[19] S.E. Csorna,[19] Z. Egyed,[19] V. Jain,[19] D. Gibaut,[20] K. Kinoshita,[20] P. Pomianowski,[20] B. Barish,[21] M. Chadha,[21] S. Chan,[21] D.F. Cowen,[21] G. Eigen,[21] J.S. Miller,[21] C. O'Grady,[21] J. Urheim,[21] A.J. Weinstein,[21] M. Athanas,[22] W. Brower,[22] G. Masek,[22] and H.P. Paar.[22]

(CLEO Collaboration)

[1]University of California, Santa Barbara, California 93106
[2]University of Colorado, Boulder, Colorado 80309-0390
[3]Cornell University, Ithaca, New York 14853
[4]University of Florida, Gainesville, Florida 32611
[5]Harvard University, Cambridge, Massachusetts 02138
[6]University of Illinois, Champaign-Urbana, Illinois, 61801
[7]Carleton University, Ottawa, Ontario K1S 5B6 and the Institute of Particle Physics, Canada
[8]McGill University, Montréal, Québec H3A 2T8 and the Institute of Particle Physics, Canada
[9]Ithaca College, Ithaca, New York 14850
[10]University of Kansas, Lawrence, Kansas 66045
[11]University of Minnesota, Minneapolis, Minnesota 55455
[12]State University of New York at Albany, Albany, New York 12222
[13]Ohio State University, Columbus, Ohio, 43210
[14]University of Oklahoma, Norman, Oklahoma 73019
[15]Purdue University, West Lafayette, Indiana 47907
[16]University of Rochester, Rochester, New York 14627
[17]Southern Methodist University, Dallas, Texas 75275
[18]Syracuse University, Syracuse, New York 13244
[19]Vanderbilt University, Nashville, Tennessee 37235
[20]Virginia Polytechnic Institute and State University, Blacksburg, Virginia, 24061
[21]California Institute of Technology, Pasadena, California 91125
[22]University of California, San Diego, La Jolla, California 92093

Abstract

We measure branching ratios for the decays $\tau^- \to K^\circ K^- \nu_\tau$ and $\tau^- \to K^\circ K^- \pi^\circ \nu_\tau$. The number of K^-'s is determined statistically from their specific ionization in the drift chamber; K°'s are identified through the $K_s \to \pi^+\pi^-$ decay. We measure $\mathcal{B}(\tau^- \to K^\circ K^- \nu_\tau) = (0.123 \pm 0.023 \pm 0.023)\%$ and $\mathcal{B}(\tau^- \to K^\circ K^- \pi^\circ \nu_\tau) = (0.129 \pm 0.050 \pm 0.032)\%$.

*Permanent address: University of Hawaii at Manoa

I. INTRODUCTION

Decays of the τ^- [1] to final states containing kaons provide information on both the SU(3) symmetry properties of the charged weak current, as well as rare decays of ρ^- and a_1^- to strange final states. Companion papers submitted to this conference [2] [3] present studies of tau decays to final states containing one and two neutral kaons. In this paper, we consider decays of tau leptons to one neutral K meson and one charged K meson.

Theoretical calculations for the processes governing these decays are limited. [4] Eidelman and Ivanchenko [5] use existing data for $e^+e^- \to \pi^+\pi^-$ and invoke conservation of the vector current (CVC) to obtain a prediction for $\tau^- \to K^\circ K^- \nu_\tau$; this approach has been very successful in matching the measured tau-decay rates for modes without kaons. Taking into account SU(3)-breaking effects such as the $\pi - K$ mass difference, they determine an expected branching ratio for $\tau^- \to K^\circ K^- \nu_\tau$ of $0.11 \pm 0.03\%$. Using a similar calculation, Narison and Pich obtain an expected value of $0.16 \pm 0.02\%$ for $\tau^- \to K^\circ K^- \nu_\tau$. [6] Decker *et al.* [7] use chiral perturbation theory to predict that the $\tau^- \to K^\circ K^- \pi^\circ \nu_\tau$ branching ratio will be substantially smaller than those for both $\tau^- \to K^- K^+ \pi^- \nu_\tau$ and $\tau \to K^\circ \bar{K}^\circ \pi^- \nu_\tau$ owing to a suppression of the K^*K component in the $K^\circ K^- \pi^\circ$ final state. Neglecting this suppression, naive isospin predicts that if both $\tau^- \to K^\circ K^- \pi^\circ \nu_\tau$ and $\tau \to K^\circ \bar{K}^\circ \pi^- \nu_\tau$ proceed through K^*K, these two branching ratios should be equal; this statement remains true even if the decay process is actually $\tau^- \to a_1^- \nu_\tau; a_1 \to K^*K$.

Experimental measurements are also sparse because of the low decay rates of the modes in question, low detection efficiency of the K°, and limited charged kaon identification capabilities of many particle detectors. The current experimental results on these decays are listed below:

$\mathcal{B}(\tau^- \to K^\circ K^- \nu_\tau) < 0.26\%$ at 95%CL (TPC)[8]
$\mathcal{B}(\tau^- \to K^\circ K^- \nu_\tau) = 0.29 \pm 0.12 \pm 0.03\%$ (ALEPH)[9]

$\mathcal{B}(\tau^- \to K^\circ K^- \pi^\circ \nu_\tau) < 0.26\%$ at 95%CL (TPC)[8]
$\mathcal{B}(\tau^- \to K^\circ K^- \pi^\circ \nu_\tau) = 0.05 \pm 0.05 \pm 0.01\%$ (ALEPH)[9]

In their measurement, the ALEPH collaboration identified K°'s based on interactions of K_L°'s in their calorimeter. CLEO identifies K°'s most efficiently using the decay $K_s^\circ \to \pi^+\pi^-$; for charged kaon identification, CLEO relies on ionization energy loss measurements (dE/dx) in the tracking chambers.

II. DATA SET

Data for this analysis are obtained with the CLEO-II detector [10] at CESR, operating at a center-of-mass energy of approximately 10.5 GeV. The data set used in this analysis comprises an integrated luminosity of 2.96fb^{-1}, corresponding to approximately 2.71×10^6 $\tau^+\tau^-$ pairs. In this analysis we measure the branching ratios of the decays $\tau^- \to K^\circ K^- \nu_\tau$ and $\tau^- \to K^\circ K^- \pi^\circ \nu_\tau$ using a sample of tau pair events selected with a 1 charged track *vs.* 3 charged track topology.

III. CALIBRATION OF DE/DX MEASUREMENT

The main 51 layer CLEO drift chamber provides dE/dx measurements with a resolution of approximately 7% for hadrons. Separation of kaons from pions based on dE/dx information is limited to momenta less than 700 MeV/c, where the separation is better than 3σ, and greater than 2.0 GeV/c, where the separation is approximately 1.6σ. Because the charged pions in the more copious decay chain $\tau^- \to K^{*-}\nu_\tau; K^{*-} \to \bar{K}^\circ\pi^-$ tend to be significantly softer than the charged kaons expected in $\tau^-\to K^\circ K^-\nu_\tau$, we will focus on the high momentum region (p_h >2 GeV/c) in this analysis to obtain a kaon-enriched sample. At CESR energies, approximately 43% of the K^- from $\tau^-\to K^\circ K^-\nu_\tau$ and 25% of the K^- from $\tau^-\to K^\circ K^-\pi^\circ\nu_\tau$, have momenta above 2.0 GeV/c. For $\tau^- \to K^\circ{}_s h^- X$ candidate events with p_{h^-} >2.0 GeV/c, [11] the K^- fraction can be determined statistically by fitting the measured dE/dx distribution for the K^- candidate. We define σ_K to be the deviation of the dE/dx measurement from that expected for true kaons at a given momentum, in units of the known resolution. We fit the σ_K distribution to two Gaussians, centered at the expected signal locations of true charged K's and π's. The means and widths of these σ_K distributions are determined from data by using $D^0 \to K^-\pi^+$ events, where the D^0 is tagged as a D^* daughter to reduce background. The σ_K distribution for these identified K's and π's is shown in Figure 1. We attribute a 6.7% systematic uncertainty to the number of K^-'s in each mode due to uncertainties in the σ_K signal parameters for K's and π's.

IV. EVENT SELECTION

Events in both modes are required to pass standard CLEO τ-pair event selection criteria. The following requirements are part of these selection criteria:

- Require that there be no more than one charged track with momentum greater than 85% of the beam energy (to reject e^+e^- and $\mu^+\mu^-$ events).
- Require that the total visible energy in the electromagnetic calorimeter be less than 85% of the total center of mass energy.
- Require that the total visible energy be greater than 20% of the total center of mass energy.

Candidate events are selected from a sample of four-charged track events with total charge zero passing the above cuts. Each event must have a reconstructed secondary vertex with a decay length of at least 5 mm and have an invariant mass within $5\sigma_{K^\circ_s}$ of the K_s mass, where $\sigma_{K^\circ_s}$ is the uncertainty in the mass, typically about 3.5 MeV.

A K^- candidate is required to be within 60° of the K° direction and have a momentum greater than 2.0 GeV/c. A 1 *vs.* 3 topology is selected by requiring an isolated track to be at least 90° from the direction of the K^- and K_s combined momentum. We require that there be either no photons in the 1-prong hemisphere or exactly two photons in this hemisphere. In the latter case the invariant mass of the photons, $M_{\gamma\gamma}$, must be within $3\sigma_{\pi^\circ}$ of the π° mass and the invariant mass of the π° and the isolated track, assumed to be a pion, must be less than 1.5 GeV. The mass resolution, σ_{π° depends on the energies and angles of the photons and is typically about 6 MeV.

V. ANALYSIS OF $\tau^-\to K^\circ K^-\nu_\tau$

A. $\tau^-\to K^\circ K^-\nu_\tau$ Event Selection

To select $\tau^-\to K^\circ K^-\nu_\tau$ events and reject background from $\tau^- \to K^\circ h^-\pi^\circ\nu_\tau$, we further require that there be no isolated photons with energy greater than 60 MeV in the signal hemisphere. To reduce background from 2-photon events we require the directional cosine of the total momentum of the event relative to the beam line be less than 0.95. Candidate events must have a vertex mass within $2\sigma_{K_s^\circ}$ of that expected for a K_s vertex and M(K_sK^-) less than the tau mass (1.777 GeV). We fit the σ_K distribution for the candidate K^- track to two Gaussians, as shown in Figure 2. The fit yields 142.1 ± 16.5 $K^\pm$ candidate events and 287.8 ± 20.6 $\pi^\pm$ candidate events. The primary source of the events with pions is the decay chain $\tau^-\to K^{*-}\nu_\tau$, $K^{*-}\to\bar{K}^\circ\pi^-\nu_\tau$. The total number of $K^\pm$ and $\pi^\pm$ events is consistent with expectations from the branching ratio measurement of Ref. [2] and the expected efficiencies for the $K^\circ K^-$ and $K^\circ\pi^-$ channels.

Events satisfying $3\sigma_{K_s^\circ} < |M_{\pi\pi} - M_{K_s}| < 5\sigma_{K_s^\circ}$ are used for background subtraction, as listed in Table 1. Hadronic background is estimated using information from the 1-prong hemisphere. The invariant mass of the isolated track and photons in the same hemisphere is determined; events with a mass greater than the tau mass are attributed to $e^+e^-\to q\bar{q}$ events and are used to estimate the hadronic background in the sample. [12] Following this procedure, we estimate the number of hadronic background events to be $20.2 \pm 8.9 \pm 15.3$. We check this number by using q$\bar{\text{q}}$ Monte Carlo; the deviation between these two hadronic background estimators is incorporated into the final systematic error. Background from B$\bar{\text{B}}$ decays is determined from Monte Carlo to be negligible.

The decay $\tau^-\to K^\circ K^-\pi^\circ\nu_\tau$ can contribute background if neither photon is observed in the signal hemisphere. A Monte Carlo study indicates that this occurs in $43 \pm 4\%$ of all such events. We use this fraction and the number of observed $\tau^-\to K^\circ K^-\pi^\circ\nu_\tau$ events (to be discussed) to estimate the feed-down from this channel to be 9.0 ± 3.0 events. A 3.0% systematic uncertainty in the overall result is attributed to this estimate. Table 1 lists the number of events in the signal region and the background estimates. (The quoted uncertainties are statistical only.)

Table 1. Number of data events and background estimates for the $\tau^-\to K^\circ K^-\nu_\tau$ analysis.

Source	Number of events
K_sK^- events in the signal region	142.1 ± 16.5
K^- events in the K_s sideband	10.0 ± 4.5
Hadronic background	20.2 ± 8.9
$\tau^-\to K^\circ K^-\pi^\circ\nu_\tau$ feed-down	9.0 ± 3.0
Signal after background subtraction	102.9 ± 19.5

B. Efficiency for Detecting $\tau^- \to K^\circ K^- \nu_\tau$

A GEANT-based [13] Monte Carlo is used to determine the efficiency for reconstructing a $\tau^- \to K^\circ K^- \nu_\tau$ event. We consider two models for $\tau^- \to K^\circ K^- \nu_\tau$. The first model assumes that the production of $K^\circ K^-$ arises entirely from high mass ρ^- decays [7] ($\rho^- \to K^\circ K^-$ model) [14] . Using this model, we find the total detection efficiency to be $(4.16 \pm 0.14)\%$. The efficiency determined from using only phase space in the $\tau^- \to K^\circ K^- \nu_\tau$ decay simulation is $(4.85 \pm 0.14)\%$; the deviation between these two values is largely due to the effect of the cut on the K^- momentum.

C. The $\tau^- \to K^\circ K^- \nu_\tau$ Invariant Mass Spectrum

We measure the $K_s K^-$ invariant mass distribution by fitting the background-subtracted σ_K distributions to two Gaussians (as described previously) in 50-MeV bins of $K_s K^-$ mass. The resulting mass distributions are shown in Figure 3. We use this distribution to determine the branching ratio for $\tau^- \to K^\circ K^- \nu_\tau$. The efficiency distributions for the two models, as a function of $K_s K^-$ mass, are shown in Figure 4. They are in rough agreement with each other. The final branching ratio is determined by performing a bin-by-bin efficiency correction to the background-subtracted $K_s K^-$ mass spectrum, and integrating. This procedure has been checked by fitting the observed data to the expected observed mass spectrum for the two separate decay models. The two signal extraction techniques give consistent results. In the latter approach, we determine the relative amounts of $\rho^- \to K^\circ K^-$ and phase space by fitting the data invariant mass distribution to the expectation of the two models (Figure 5). We find that an approximately equal contribution of phase space and $\rho^- \to K^\circ K^-$ models provides the best fit to the data. A more complete analysis taking into account relevant systematic errors is in progress.

The branching ratio we obtain for this decay mode is

$$\mathcal{B}(\tau^- \to K^\circ K^- \nu_\tau) = (0.123 \pm 0.023 \pm 0.023)\%,$$

in good agreement with the CVC-derived predictions of Ref. [5-6].

D. Systematic Uncertainties

The major contributions to the systematic uncertainty are discussed in the preceding sections. These and the systematic uncertainties due to K_s reconstruction, charged particle tracking, and photon finding are listed in Table 2.

VI. $\tau^- \to K^\circ K^- \pi^\circ \nu_\tau$ ANALYSIS

A. $\tau^- \to K^\circ K^- \pi^\circ \nu_\tau$ Event Selection and Signal Determination

To isolate $\tau^- \to K^\circ K^- \pi^\circ \nu_\tau$ events we require that there be exactly two isolated photons, with energy greater than 90 MeV in the $K_s K^-$ hemisphere. Signal and sideband regions are

Table 2. Estimate of systematic uncertainties for $\tau^- \to K^\circ K^- \nu_\tau$

Cause	Error (%)
Non-τ Background	12.0
Model	8.0
σ_K uncertainties	6.7
Charged particle tracking	5.2
K_s finding	5.0
Photon finding	4.0
Monte Carlo statistics	3.1
$\tau^- \to K^\circ K^- \pi^\circ \nu_\tau$ feed-down	3.0
Total	18.4

defined as $|M_{\gamma\gamma} - M_{\pi^\circ}| < 2\sigma_{\pi^\circ}$ and $4\sigma_{\pi^\circ} < |M_{\gamma\gamma} - M_{\pi^\circ}| < 6\sigma_{\pi^\circ}$, respectively. The plot of $M_{\gamma\gamma}$ *vs.* $M_{\pi\pi}$ is shown in Figure 6. The signal region lies within the solid box; the signal and sideband regions are also indicated. From the sideband regions we estimate a background of 2$\pm$2 events in the signal region. The fit of the σ_K distribution for the K^- candidate track to two Gaussians (Figure 7) yields $N(K^-) = 30.2 \pm 7.2$ events and $N(\pi^-) = 28.1 \pm 7.1$ events for which $M(K_s K^- \pi^\circ) < M_\tau$. There are 3.0 events with $M(K_s K^- \pi^\circ) > M_\tau$ and h^- consistent with being a K^- meson. From this we estimate that there are $6.0 \pm 4.0 \pm 6.0$ hadronic background events in the $\tau^- \to K^\circ K^- \pi^\circ \nu_\tau$ sample. The total number of $K^\pm \pi^\circ$ and $\pi^\pm \pi^\circ$ events is consistent with expectations from the branching ratio measurement of Ref. [2] and the expected efficiencies for the $K^\circ K^- \pi^\circ$ and $K^\circ \pi^- \pi^\circ$ channels.

Table 3 lists the number of events in the signal region and the corresponding backgrounds. Monte Carlo studies indicate that feed-up from $\tau^- \to K^\circ K^- \nu_\tau$ is negligible. We also assume that the branching ratios to states with additional π°'s are negligible.

Table 3. Number of data events and background estimates for the $\tau^- \to K^\circ K^- \pi^\circ \nu_\tau$ analysis.

Source	Number of events
$K_s K^- \pi^\circ$ events in the signal region	30.2 ± 7.2
K^- events in the K_s & π° sidebands	2.0 ± 2.0
Hadronic background	6.0 ± 4.0
Signal after background subtraction	22.2 ± 8.5

B. The $\tau^- \to K^\circ K^- \pi^\circ \nu_\tau$ Invariant Mass Spectrum

The invariant mass distribution of $\tau^- \to K^\circ K^- \pi^\circ \nu_\tau$ candidates is obtained by using the same technique as was described in section **V.C**, by fitting the σ_K distributions in bins of $\tau^-\to K^\circ K^-\pi^\circ\nu_\tau$ mass. Figure 8 shows the invariant mass distribution for the $\tau^-\to K^\circ K^-\pi^\circ\nu_\tau$ candidates.

C. Efficiency for Detecting $\tau^-\to K^\circ K^-\pi^\circ\nu_\tau$

To extract the branching ratio for $\tau^-\to K^\circ K^-\pi^\circ\nu_\tau$, we must once again take into account the mass dependence of the detection efficiency. We study the efficiency in the Monte Carlo for two decay models: $\tau\to K^*K\nu_\tau$, proceeding through the decay $a_1\to K^*K$; and $\tau\to\rho\pi\nu_\tau$ with the ρ^- decaying to $K^\circ K^-$. The $\tau\to K^*K\nu_\tau$ decays are generated with equal amounts of $K^{*-}K^\circ$ and $K^{*\circ}K^-$. Both of these models are implemented in KORALB as described in Ref. [7]. The integrated efficiencies for the K^*K and $\rho^-\to K^\circ K^-$ models are $0.87\pm0.05\%$ and $0.80\pm0.04\%$, respectively. As in the $\tau^-\to K^\circ K^-\nu_\tau$ analysis we determine the relative contribution of each model by fitting the data mass distributions to admixtures of the two Monte Carlo distributions. The fit prefers $\tau\to K^*K\nu_\tau$ with very little admixture of the $\rho^-\to K^\circ K^-$ model. Fits to the $K^-\pi^\circ$ and $K_s\pi^\circ$ mass distributions (Figures 9 and 10, respectively) are also consistent with the conclusion that 100% $\tau\to K^*K\nu_\tau$ can adequately describe the data. This is qualitatively in agreement with the study of the $\tau^-\to K^o_s K^-{}^o_s\pi^-\nu_\tau$ final state reported at this conference [2]. Further quantitative studies of the mass distribution, including systematic errors, are in progress.

As before, we determine the branching ratio by integrating the efficiency corrected $K_sK^-\pi^\circ$ mass distribution and check this by fitting the shape given by the $\tau\to K^*K\nu_\tau$ Monte Carlo. These techniques give consistent results. As before, the deviation between the efficiency estimates for the two models is taken to be the systematic error due to model dependence.

The branching ratio we determine for this mode is

$$\mathcal{B}(\tau^-\to K^\circ K^-\pi^\circ\nu_\tau) = 0.129\pm0.050\pm0.032.$$

D. Systematic Uncertainties

The major contributions to the systematic uncertainty are discussed in the preceding sections. These and the systematic uncertainties due to K_s reconstruction, charged particle tracking, and photon finding are listed in Table 4.

VII. CONCLUSIONS

We observe a convincing signal for the decays $\tau^-\to K^\circ K^-\nu_\tau$ in the σ_K distribution for K^- momentum above 2.0 GeV/c and a smaller signal for $\tau^-\to K^\circ K^-\pi^\circ\nu_\tau$. We measure the branching ratios

$$\mathcal{B}(\tau^-\to K^\circ K^-\nu_\tau) = 0.123\pm0.023\pm0.023$$

$$\mathcal{B}(\tau^-\to K^\circ K^-\pi^\circ\nu_\tau) = 0.129\pm0.050\pm0.032.$$

Table 4. Estimate of systematic uncertainties for $\tau^- \to K^\circ K^- \pi^\circ \nu_\tau$

Cause	Error (%)
Non-τ Background	20.0
Model	8.0
σ_K uncertainties	6.7
Monte Carlo statistics	5.5
Charged particle tracking	5.2
K_s finding	5.0
Photon finding	5.0
π° reconstruction	3.0
Total	25.0

Our results represent the most precise values for these branching ratios obtained to date. Given the errors, our numbers are not inconsistent with those of the ALEPH collaboration. However, the indication from the ALEPH results that $\tau^- \to K^\circ K^- \nu_\tau$ is substantially larger than $\tau^- \to K^\circ K^- \pi^\circ \nu_\tau$ is not supported by our data. The result for $\tau^- \to K^\circ K^- \nu_\tau$ is in good agreement with the CVC-derived predictions of Ref. [5-6]. Preliminary results of the fits to the mass spectra for the $K^\circ K^- \pi^\circ$ final state are consistent with those expected from $\tau^- \to K^* K \nu_\tau$. This preliminary result, as well as the numerical consistency of our branching ratio with that measured for $\tau \to K^\circ \bar{K}^\circ \pi^- \nu_\tau$, are at variance with the prediction of Ref. [7].

ACKNOWLEDGEMENTS

We gratefully acknowledge the effort of the CESR staff in providing us with excellent luminosity and running conditions. J.P.A. and P.S.D. thank the PYI program of the NSF, I.P.J.S. thanks the YI program of the NSF, G.E. thanks the Heisenberg Foundation, K.K.G., I.P.J.S., and T.S. thank the TNRLC, K.K.G., H.N.N., J.D.R., T.S. and H.Y. thank the OJI program of DOE and P.R. thanks the A.P. Sloan Foundation for support. This work was supported by the National Science Foundation, the U.S. Dept. of Energy and the Natural Sciences and Engineering Research Council of Canada.

REFERENCES

[1] Throughout this paper charge-conjugate states are also included.

[2] M. Athanas *et al.*, (CLEO-II Collaboration), *Study of the Decays* $\tau^- \to \mathbf{K^\circ{}_s h^-}(\pi^\circ)\nu_\tau$, CLEO CONF 94-23, contributed paper GLS0460, submitted to this conference.

[3] R. Balest *et al.*, (CLEO-II Collaboration), *Observation of Tau Decays with Two Neutral Kaons*, CLEO CONF 94-25, contributed paper GSL04555, submitted to this conference.

[4] F.J. Gilman and S.H. Rhie, Phys. Rev. D **31**, 1066 (1985).

[5] S.I. Eidelman and V.N. Ivanchenko, Phys. Lett. **B257**, 437, (1991).

[6] S. Narison and A. Pich, Phys. Lett. **B**304, 359 (1993).

[7] R. Decker, E. Mirkes, R. Sauer, and Z. Was, Z. Phys. C**58**, 445 (1993).

[8] H. Aihara *et al.*, (TPC/2γ Collaboration), Phys. Rev. Lett. **59**, 751 (1987).

[9] D. Buskulic *et al.*, (ALEPH Collaboration), CERN-PPE/94-59, April 1994.

[10] Y. Kubota *et al.*, (CLEO-II Collaboration), Nucl. Instrum. Methods A **320**, 66 (1992).

[11] This is essentially the same event sample used in reference [1], with the added momentum requirement on the three-prong charged hadron not associated with the secondary vertex.

[12] This procedure is described in M. Procario *et al.*, (CLEO-II Collaboration), Phys. Rev. Lett. **70**, 1207 (1993).

[13] R. Brun *et al.*, GEANT 3.14, CERN DD/EE/84-1.

[14] We put in spin correlations between the two kaons in the final state as expected for, e.g., $\tau^- \to \pi^-\pi^\circ$, as implemented in the KORALB tau-decay event generator. In particular, the angular decay distribution of the K^-K° system is specified by taking this system to be in a vector state. The mass spectral function is modelled using a form factor derived from fits to $e^+e^- \to \pi^+\pi^-$ data, which has been shown to describe well the $\tau^- \to \pi^-\pi^\circ\nu_\tau$ spectral function. See J. Kühn and A. Santamaria, Z. Phys. C**48**, 443 (1990).

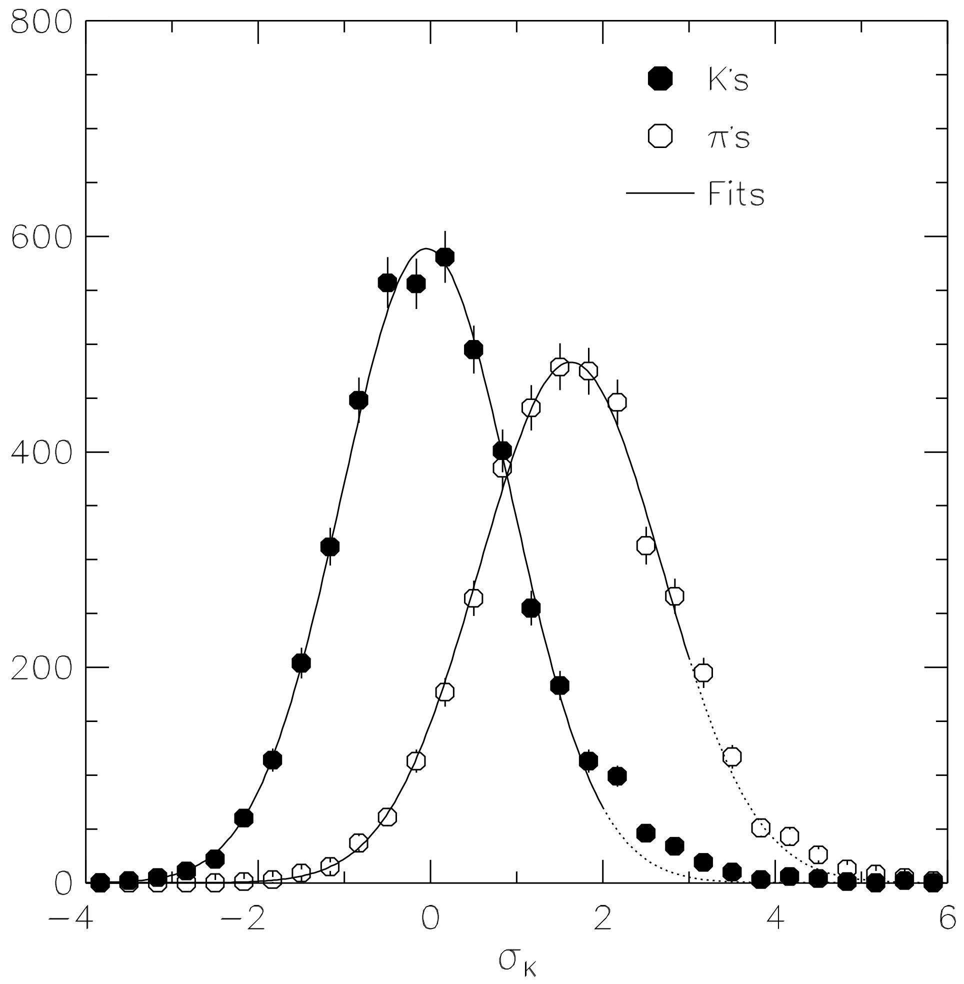

FIG. 1. The σ_K distributions of $K^{\pm}$ meson candidates (filled circles) and $\pi^{\pm}$ candidates (open circles) from $D^{*\pm}$ decays. The solid lines show the fit of each distribution to a Gaussian.

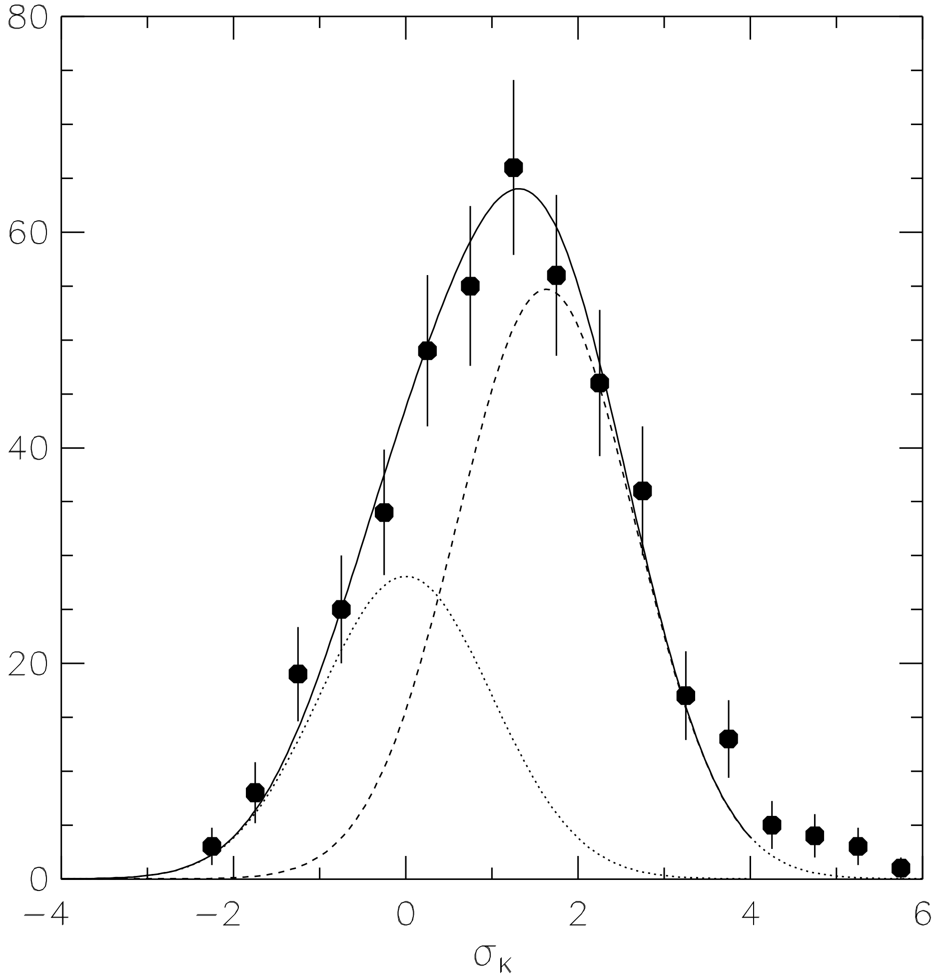

FIG. 2. The σ_K distributions for K^- candidates from $\tau^- \to K^\circ K^- \nu_\tau$ decays. The points are from data, the solid line shows the fit to two Gaussians, the dotted line is the Gaussian consistent with the K hypothesis, and the dashed line is the Gaussian consistent with the π hypothesis. Points above 4.0 are excluded from the fit.

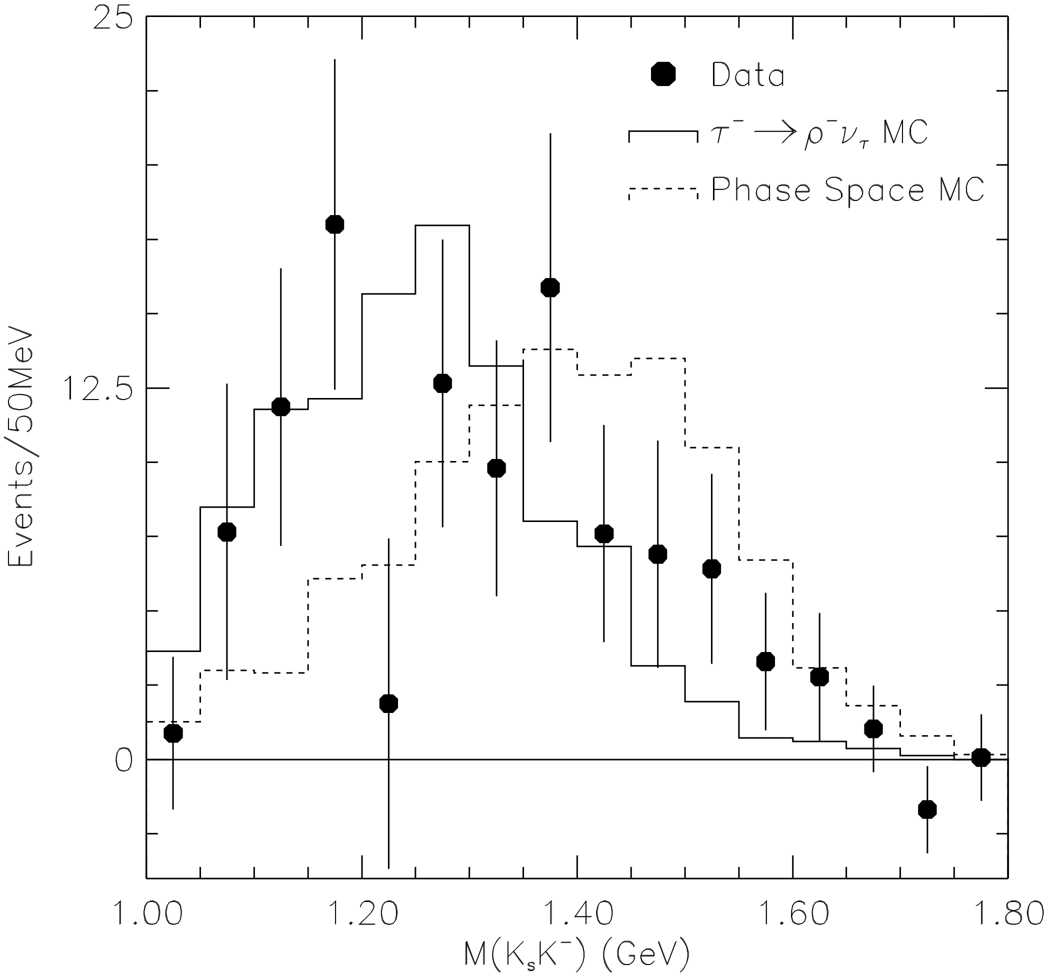

FIG. 3. The K_sK^- invariant mass distribution from $\tau^-\to K^\circ K^-\nu_\tau$ candidates. The solid histogram shows the invariant mass spectrum from a full Monte Carlo simulation of $\tau^-\to\rho^-\nu_\tau$, $\rho\to K_sK^-$. The dashed histogram shows the mass distribution from the phase space Monte Carlo.

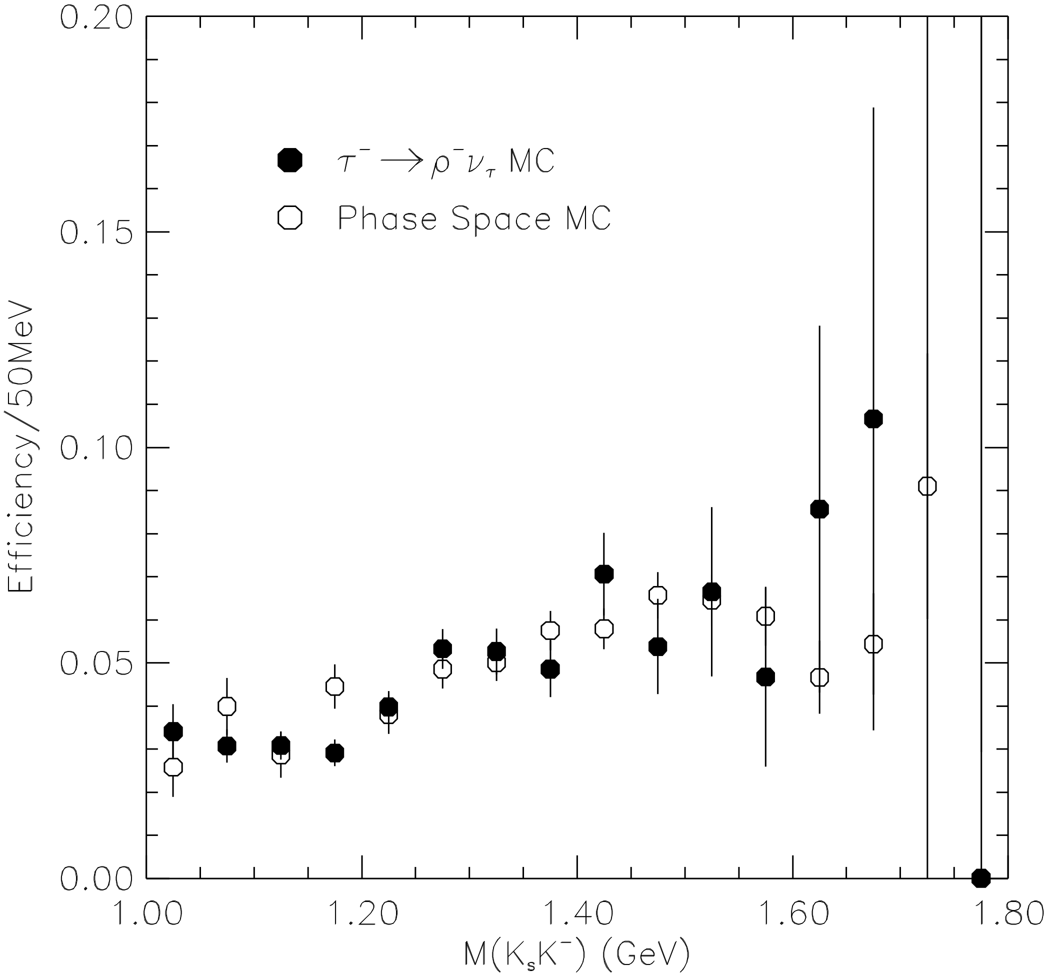

FIG. 4. The $\tau^- \rightarrow K^\circ K^- \nu_\tau$ detection efficiency versus $K_s K^-$ invariant mass. The filled circles are from fully simulated $\tau^- \rightarrow \rho^- \nu_\tau$, $\rho \rightarrow K_s K^-$ decays. The open circles are from a $\tau^- \rightarrow K^\circ K^- \nu_\tau$ phase space Monte Carlo.

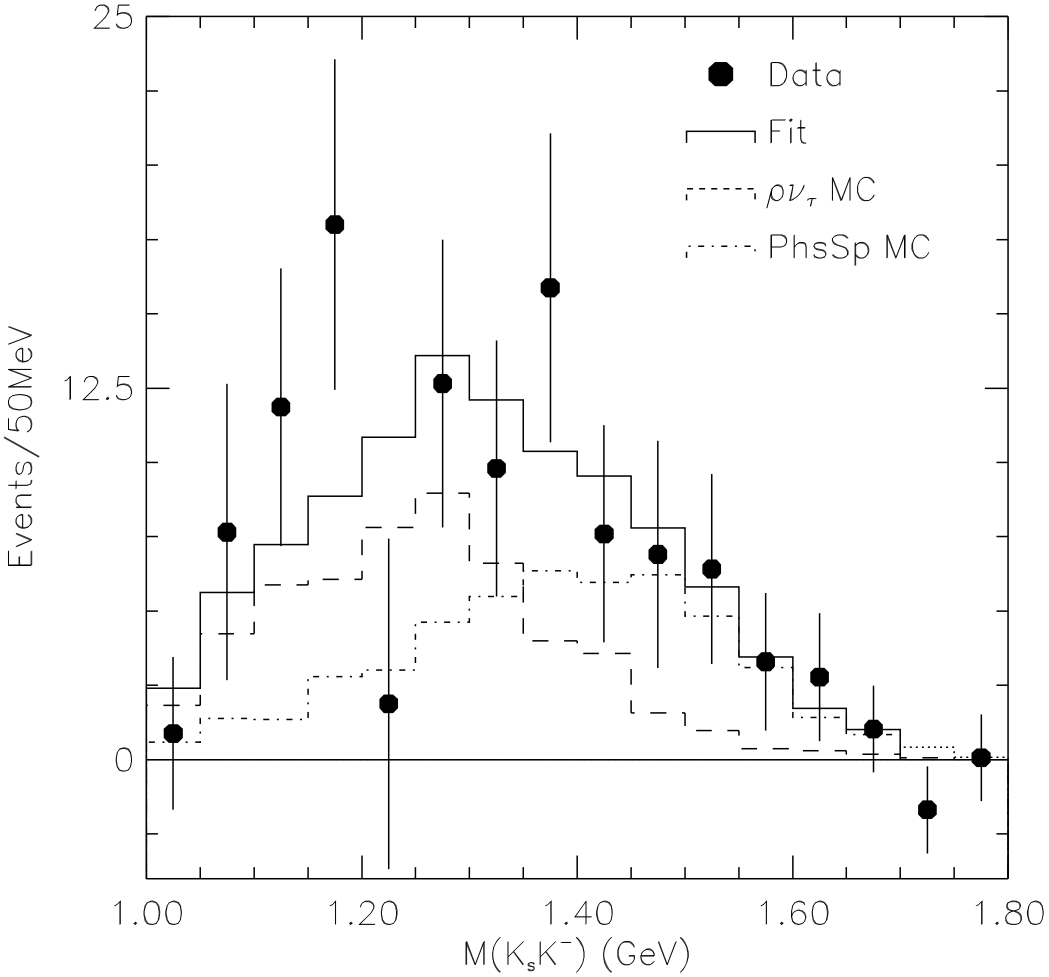

FIG. 5. The K_sK^- invariant mass of $\tau^-\to K^\circ K^-\nu_\tau$ events. The filled circles, with error bars, are for the data. The solid histogram is the result of a fit to the sum of $\tau^-\to\rho^-\nu_\tau$, $\rho\to K_sK^-$ (dashed) and $\tau^-\to K^\circ K^-\nu_\tau$ phase space (dot-dashed) Monte Carlo models.

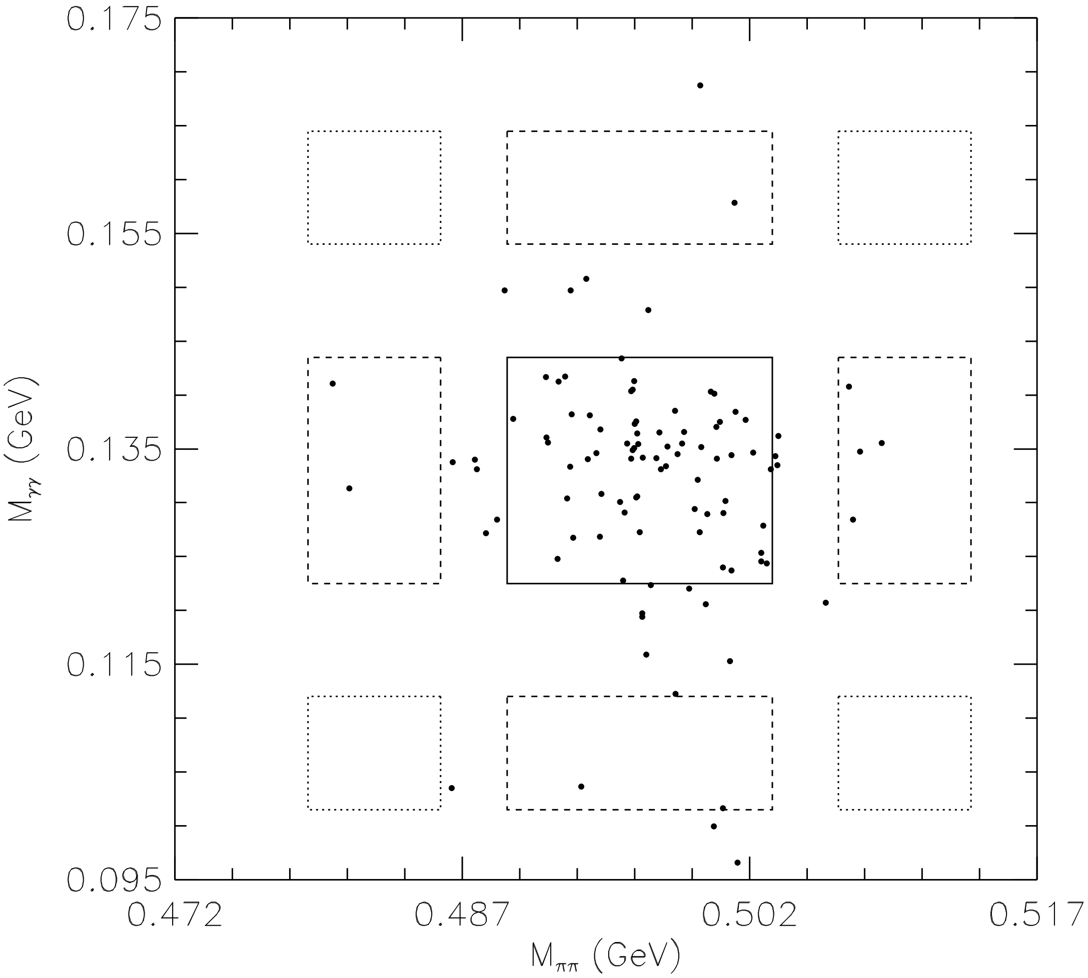

FIG. 6. Plot of $M_{\gamma\gamma}$ *vs.* $M_{\pi\pi}$ for $\tau^- \rightarrow K^\circ K^- \pi^\circ \nu_\tau$ candidates. The solid box indicates the signal region where both masses are within 2σ of their expected values. The dashed and dotted boxes indicate the sideband regions.

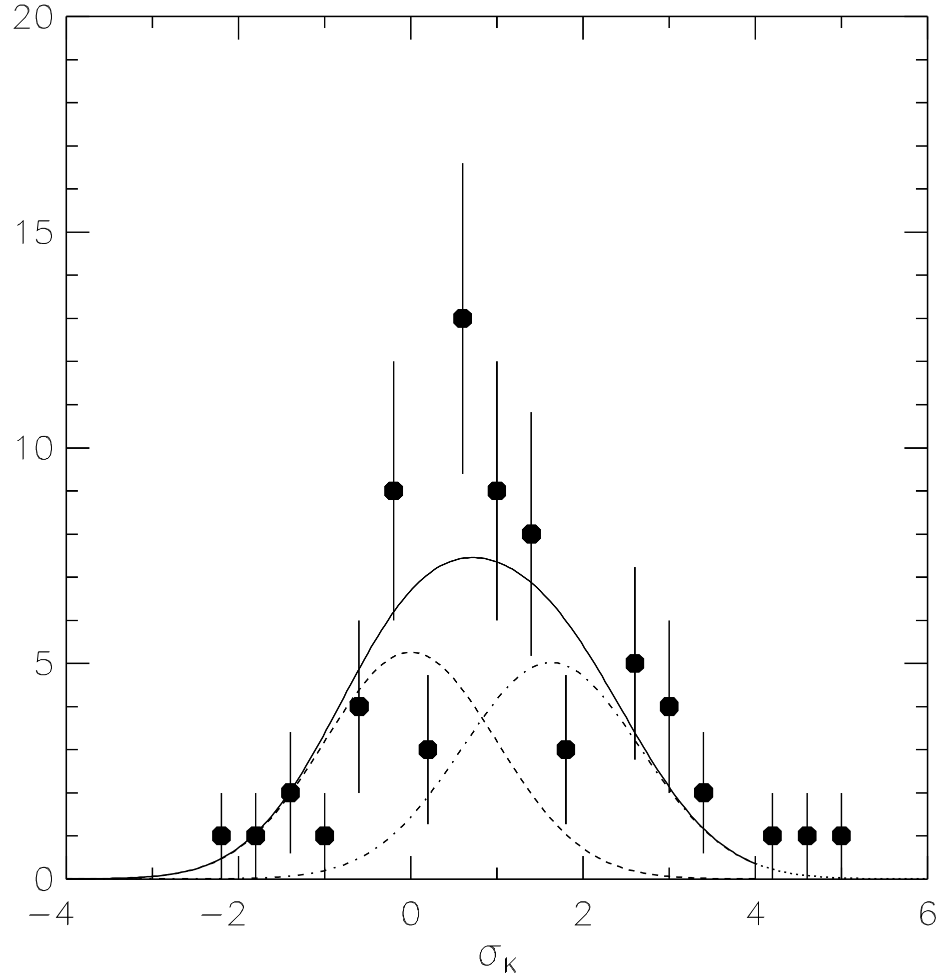

FIG. 7. The distribution of the variable σ_K (see text) for K^- candidates from $\tau^- \to K^\circ K^- \pi^\circ \nu_\tau$ decays. The points are from data, the dashed (dot-dashed) curve is from the K^- (π^-) component of the fit to two Gaussians, and the solid curve is their sum. Points above 4.0 are excluded from the fit.

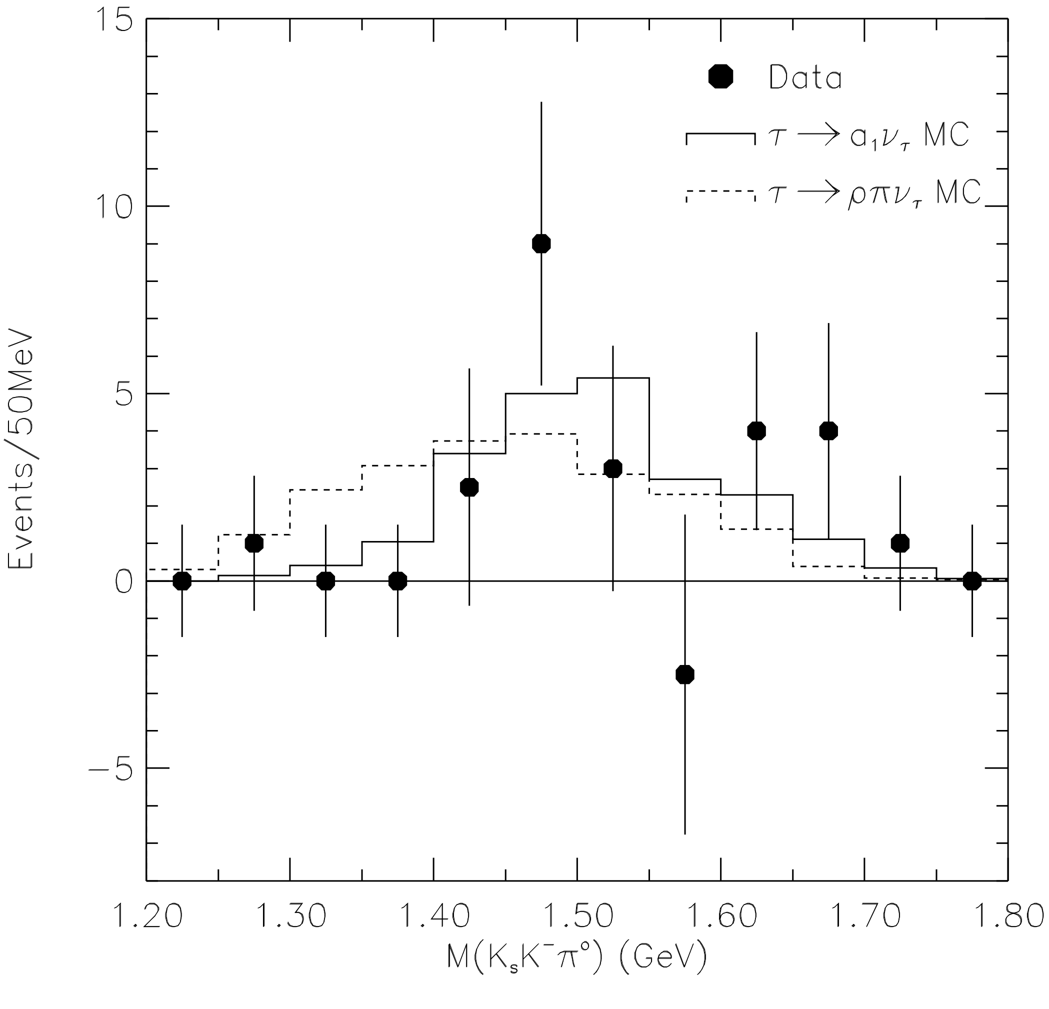

FIG. 8. The $K_sK^-\pi^\circ$ invariant mass distribution for $\tau^-\to K^\circ K^-\pi^\circ\nu_\tau$ candidates. The data points are obtained by taking 50 MeV "slices" in invariant mass and fitting the background subtracted σ_K distribution for those events. The solid histogram shows the invariant mass spectrum from a full Monte Carlo simulation of $\tau^-\to a_1\nu_\tau,\ a_1\to K^*K$ decays. The dashed histogram shows the mass distribution for a simulation of $\tau^-\to\rho\pi\nu_\tau,\ \rho\to K^\circ K^-$ decays.

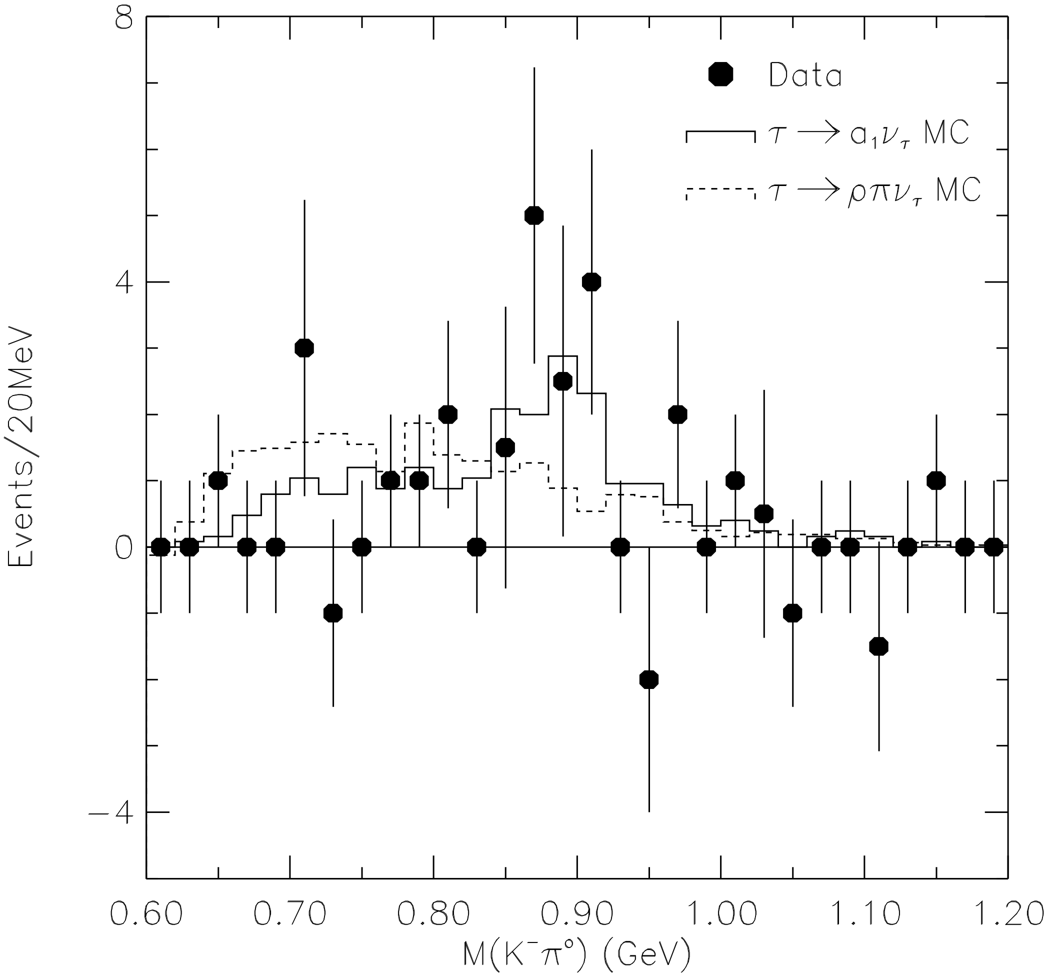

FIG. 9. The $K^-\pi^\circ$ invariant mass distribution for $\tau^-\to K^\circ K^-\pi^\circ\nu_\tau$ candidates. The solid histogram shows the invariant mass spectrum from a full Monte Carlo simulation of $\tau^-\to a_1\nu_\tau$, $a_1\to K^*K$ decays. The dashed histogram shows the mass distribution from a simulation of $\tau^-\to\rho\pi\nu_\tau$, $\rho\to K^\circ K^-$ decays.

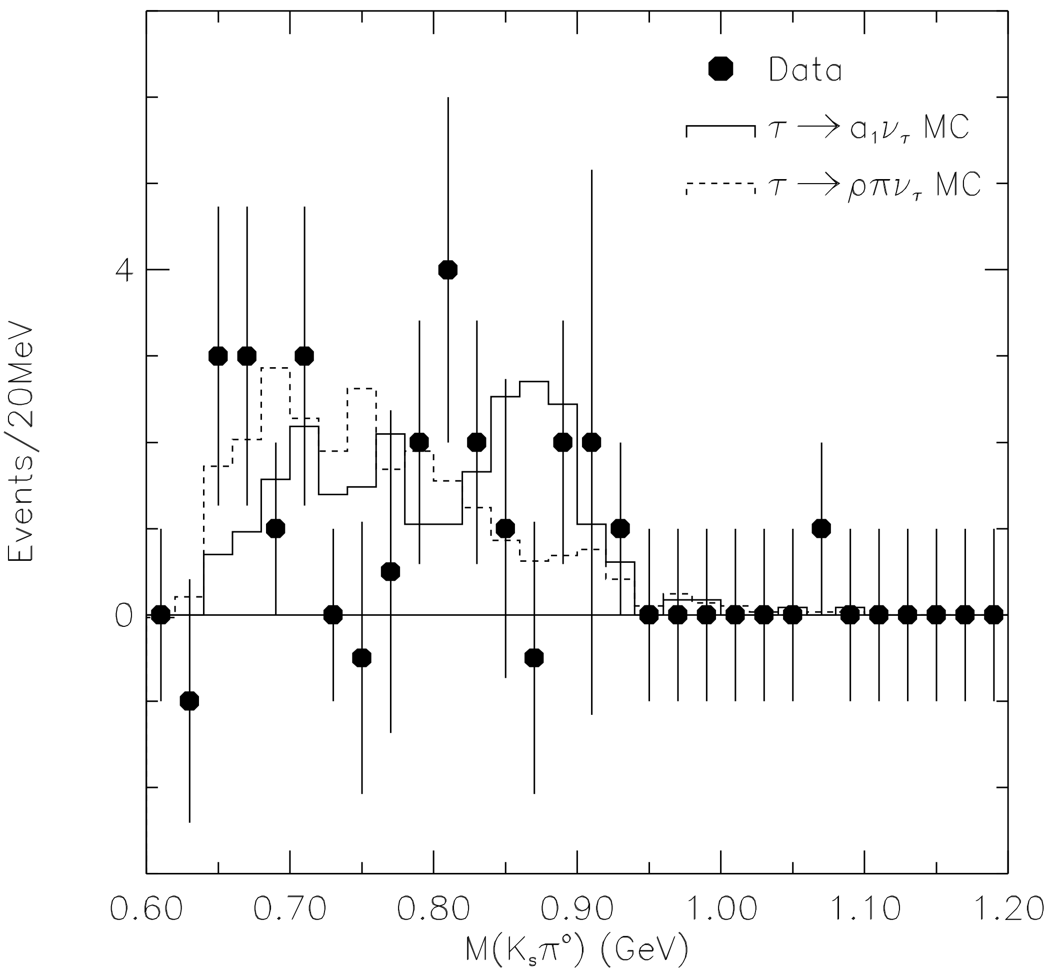

FIG. 10. The $K_s\pi^\circ$ invariant mass distribution for $\tau^-\!\rightarrow K^\circ K^-\pi^\circ\nu_\tau$ candidates. The solid histogram shows the invariant mass spectrum from a full Monte Carlo simulation of $\tau^-\!\rightarrow a_1\nu_\tau$, $a_1\!\rightarrow K^*K$ decays. The dashed histogram shows the mass distribution for a simulation of $\tau^-\!\rightarrow\rho\pi\nu_\tau$, $\rho\!\rightarrow K^\circ K^-$ decays.